Pulsed Gradient Spin Echo Nuclear Magnetic Resonance Imaging of Diffusion in Granular Flow

Joseph D. Seymour, Arvind Caprihan, Stephen A. Altobelli, and Eiichi Fukushima
New Mexico Resonance, 2425 Ridgecrest Drive SE, Albuquerque, New Mexico 87108
(Received 3 March 1999)

We derive the formalism to obtain spatial distributions of collisional correlation times for macroscopic particles undergoing granular flow from pulsed gradient spin echo nuclear magnetic resonance diffusion data. This is demonstrated with an example of axial motion in the shear flow regime of a 3D granular flow in a horizontal rotating cylinder at one rotation rate.

PACS numbers: 45.70.Mg, 76.60.Pc

Granular flow phenomena have engendered interdisciplinary interest due to their behavior encompassing solidlike, fluidlike, and gaslike states [1]. They have important applications in the food, chemical, power, and pharmaceutical industries, as well as in the analysis of avalanche danger and mitigation. Their complex behavior includes pattern formation in vibrating systems [2] and particle segregation in rotating drums [3]. Enhanced understanding of granular dynamics is technologically relevant and can even provide insight into astrophysics and statistical mechanics [1].

The scarcity of detailed experimental data, caused mainly by an absence of good techniques to study motions inside the flow, forms a major barrier to a better understanding of these flows. Nuclear magnetic resonance (NMR) is a unique tool that yields not only static but also dynamic variables such as velocity [4], and it has recently been applied to granular flows [5,6]. Most NMR studies image the spin density, i.e., particle concentration, while the sample is at rest, as is done between shakes [7,8], and to follow the evolution of segregation in rotating granular flow [3]. Spin density measurements during motion, though more difficult, have been reported for vibrating beds [9] and rotating cylinders [5,6].

Despite perceived difficulties of applying PGSE (pulsed gradient spin echo) NMR [4] to granular flows [8], PGSE imaging can display the spatial distribution of correlation times in granular flow. This is accomplished by measuring both deterministic and random particle dynamics of granular flow in a horizontal rotating cylinder for a specified observation window that is comparable to the correlation time. We will consider only a small set of parameters because of space limitations; however, the extension of the technique to obtain full flow information will become clear, later.

To date, there have been only preliminary applications of PGSE NMR to granular materials [5,6]. Other techniques to measure particle diffusion are NMR tagging for single shakes [8], time series photographs [10,11], and diffusing-wave spectroscopy [12]. The first two methods measure total displacements after few or many collisions, while the latter provides statistics of particle displacements within 3D granular flows for a limited depth, without providing spatial distributions or anisotropies in the diffusive motion. Hence, our measurements are unique to be able to spatially resolve potentially anisotropic microscopic motions.

The theories of Brownian motion and kinetic theory have been used to model velocity fluctuations in granular shear flows [13]. The asymptotic diffusion coefficient is

$$D = \frac{1}{3}\int_0^\infty \langle \mathbf{u}(t)\cdot\mathbf{u}(0)\rangle\, dt = \frac{a\sqrt{\pi T}}{8(1+e)\nu g_0(\nu)}, \quad (1)$$

where the fluctuation velocity $\mathbf{u} = \mathbf{v} - \langle\mathbf{v}\rangle$ with particle point velocity $\mathbf{v}$ and mean velocity $\langle\mathbf{v}\rangle$, a the particle diameter, $T = 1/3\langle u^2\rangle$ granular temperature, e the coefficient of restitution, ν the solids fraction, and $g_0(\nu)$ the radial distribution function at contact. Equation (1) is derived assuming an exponential velocity fluctuation autocorrelation function, $\langle\mathbf{u}(t)\cdot\mathbf{u}(0)\rangle = \langle u^2\rangle\exp(-t/\tau_c)$ [13], true for a stationary Gaussian Markov Ornstein-Uhlenbeck (O-U) process for the velocity of a particle with velocity fluctuation correlation time τ_c.

We will use NMR sequences that are based on PGSE [14], adapted to imaging. The PGSE signal is the characteristic functional of the stochastic process due to its Fourier relationship with the propagator of the motion. It is given by $E(t) = \langle\exp[i\phi(t)]\rangle = \exp[i\langle\phi(t)\rangle]\exp[-\alpha(t)]$ [4,15,16], where the cumulant expansion [17] is applied and the brackets $\langle\bullet\rangle$ represent an ensemble average of spins in a volume element. Magnetization mean phase $\langle\phi(t)\rangle$ within the ensemble depends on the average motion of the spins along the applied gradient $g(t)$, taken to be along z. A Taylor series of the spin position $z(t)$ relates the phase $\langle\phi(t)\rangle = \gamma[z_0 m_0 + \langle\nu_z\rangle m_1 + \langle a_z\rangle m_2 + \ldots]$ to initial position z_0, mean velocity $\langle\nu_z\rangle$, and mean acceleration $\langle a_z\rangle$, through temporal moments of the applied motion-sensitizing gradients $m_n = (1/n!)\int_0^t t^n g(t')\,dt'$. In the repeated PGSE experiment [Fig. 1(a)] the zeroth gradient moment m_0 is nulled and the phase shift of the magnetization is sensitive to mean velocity $\langle\nu_z\rangle$ while in flow compensated PGSE [Fig. 1(b)] the zeroth and first gradient moments m_0 and m_1 are nulled and the magnetization phase is modulated due to mean acceleration $\langle a_z\rangle$.

 0031-9007/00/84(2)/266(4)$15.00

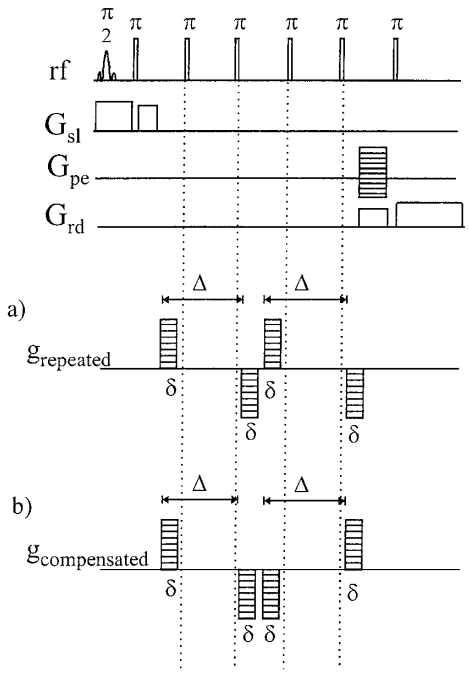

FIG. 1. Sequence of radio frequency (rf) and magnetic field gradient pulses for imaging the spatial distribution of motion. (a) Velocity sensitive repeated PGSE sequence; (b) velocity compensated PGSE sequence. An even echo is required for both experiments in order to refocus the spins diffusing in inhomogeneous background magnetic fields. Use of multiple π pulses permits measurements with $\Delta > T_E$, where T_E is the time between π pulses.

The attenuation of the PGSE signal to second order is [4,15,16]

$$\alpha(t) = \frac{1}{\pi} \int_0^t D_{zz}(\omega)\, |F(\omega, t)|^2\, d\omega\,. \qquad (2)$$

$D_{zz}(\omega) = \int_0^\infty \langle u(t)u(0)\rangle e^{i\omega t}\, dt$ is the zz component of the self-diffusion tensor, which is the Fourier transform of the velocity fluctuation autocorrelation, and $F(\omega, t) = \int_0^t [\gamma \int_0^{t'} g(t'')\, dt'']e^{i\omega t'}\, dt'$ is the spectrum of the motion-encoding gradient. For a gradient pulse of amplitude g and duration δ, separated by displacement time Δ and constant diffusion coefficient D_{zz}, one obtains the Stejskal-Tanner result $\alpha(t) = 4\pi^2 q^2 D_{zz}(\Delta - \delta/3)$, where $q = (2\pi)^{-1}\gamma g \delta$ [4,16]. Truncation at second order is equivalent to a Gaussian velocity fluctuation that is consistent with the O-U process [17] model of diffusion in granular shear flows [13]. It applies here because we obtain the diffusion coefficient from the long displacement length NMR data in the low-q limit, where the cumulant expansion is approximately Gaussian regardless of the form of the complete propagator [16]. The diffusion coefficient in Eq. (1) is that of Eq. (2) in the long time limit, $D_{zz}(0) = \lim_{t\to\infty} \frac{\langle Z^2\rangle}{2t}$, where $\langle Z^2\rangle$ is the displacement variance.

Following Savage and Dai [13], we apply the O-U process model for velocity fluctuations to granular flow. From Eq. (2), the repeated PGSE signal attenuation is [4,16]

$$\alpha(t) = 4\pi^2 q^2 (\tfrac{1}{2}\langle u_z^2\rangle)\Delta^2, \qquad D = \tfrac{1}{2}\langle u_z^2\rangle\Delta\,, \quad \tau_c > \Delta\,, \qquad (3a)$$

$$\alpha(t) = 4\pi^2 q^2 (\langle u_z^2\rangle\tau_c)(\Delta - \delta/3), \qquad D = \langle u_z^2\rangle\tau_c\,, \quad \tau_c \ll \Delta\,, \qquad (3b)$$

whereas the compensated PGSE signal would not attenuate, i.e., $\alpha(t) = 0$, for $\tau_c > \Delta$ but be identical with (3b) for $\tau_c \ll \Delta$ [4]. We call D the effective diffusion coefficient because the motion is Brownian only when $\tau_c \ll \Delta$. Otherwise, the collisions are not frequent enough to be statistically random. In this work, the correlation time τ_c is assumed to be the time between particle collisions [12] that cause velocity changes in the direction of the applied motion-sensitizing magnetic field gradient.

When $\tau_c > \Delta$, we have an O-U process with ballistic motion in the stationary random flow regime [4] *during the time* Δ. When $\tau_c \ll \Delta$, the motion is in the pseudodiffusion limit [17] due to multiple collisions in time Δ. The repeated PGSE experiment [Fig. 1(a)] yields an effective diffusion coefficient D for the O-U process with particles having all values of τ_c. In contrast, compensated PGSE [Fig. 1(b)] refocuses magnetization due to the spins that remain coherent during Δ, so the signal attenuation would be caused only by those particles with τ_c of the order of or less than Δ.

Thus, we are able to study the statistical nature of the motion in a time window Δ that is experimentally adjustable, i.e., the motion will be deterministic if the correlation time is longer than the window, whereas the motion will look random if the correlation time is much shorter than the window. The collisional correlation time, which is a major microscopic parameter in granular flow studies, can then be characterized by studying the dynamics as a function of the duration Δ.

The system studied was a 70 mm inside diameter, 245 mm long acrylic cylinder half full of 2 mm diameter oil-filled plastic beads. The rotation rate reported here is 2.36 rad s^{-1} and the flow occurs in a lens-shaped region near the flat free surface [5]. The rotation carries particles around as a solid body up to the flowing region where mean flow occurs nearly parallel to the free surface. Each particle accelerates and decelerates relatively symmetrically about the center of the flowing motion before returning to the solid body region. The average flow is two dimensional with no mean axial velocity within the resolution of the repeated PGSE experiment of 7.4×10^{-3} m s^{-1} and no mean axial acceleration to within 1 m s^{-2} as measured by compensated PGSE. Only diffusive motion in a 20 mm thick slice perpendicular to the cylinder axis near the center of the cylinder will be reported.

Figure 2 shows Stejskal-Tanner plots for axial motion in two pixels, one in the lower half of the flowing region [Fig. 2(a)] and the other in the upper half [Fig. 2(b)], both

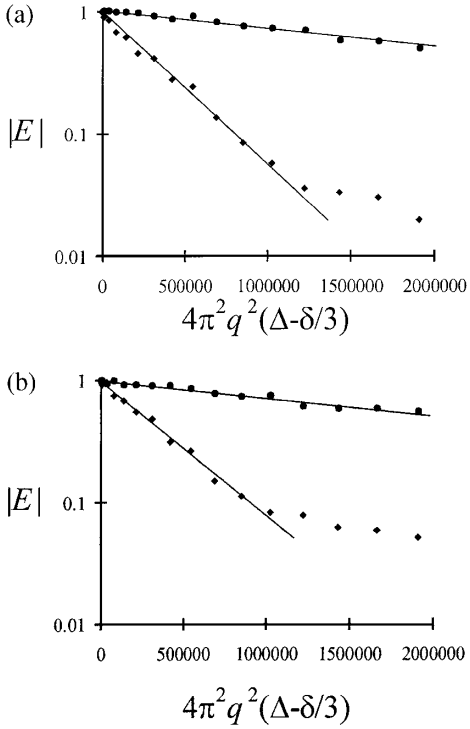

FIG. 2. Echo attenuation amplitude (Stejskal-Tanner) plots. Linear fits to the low-q, long range displacement data provide the effective diffusion coefficient to generate images as in Fig. 3. Data are for two voxels near the surface of the flowing region in the (a) lower and (b) upper half of flow. Observation time is $\Delta = 2.58$ ms. Motion sensitivity is in the axial direction where no net flow is measured. The repeated PGSE data (◆) exhibit greater attenuation than the compensated PGSE data (●).

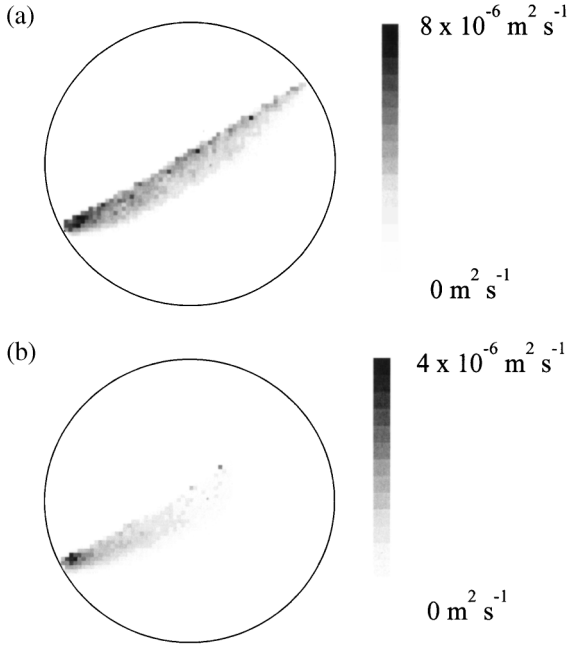

FIG. 3. NMR images of axial effective diffusion coefficient for repeated (a) and compensated (b) PGSE at a rotation rate of 2.36 rad s^{-1}. Spatial resolution in the transverse (r, θ) plane of the cylinder is 1 mm $\times$ 1 mm with a 20 mm thick axial slice. Note the factor of 2 difference in the scaling between (a) and (b). The larger effective diffusion in (a) indicates the presence of particle motions correlated on time scales longer than $\Delta = 6.54$ ms in the axial direction. Correlated motions that cause spin dephasing for the repeated PGSE experiment are refocused in the compensated PGSE experiment, yielding a smaller effective diffusion due only to random motion.

3 mm below the surface. The plots are linear in the low-q regime, indicating Gaussian behavior, consistent with exponential velocity fluctuation correlation. The compensated PGSE data (●) show nonzero attenuation indicating the presence of random motion within the time frame of $\Delta = 2.58$ ms, whereas the difference between the two curves indicates a nonrandom motion superposed on the random motion. This point is supported by the biexponential decay in Fig. 2 for the repeated PGSE data, in which the slope of the higher q data is similar to the slope of the compensated PGSE [4].

Figures 3(a) and 3(b), respectively, show transverse slices of effective axial diffusion coefficient measured with repeated and compensated PGSE experiments for $\Delta = 6.54$ ms at a cylinder rotation rate of 2.36 rad s^{-1}. Effective axial diffusivities from repeated PGSE are a factor of 2 greater than from compensated PGSE, indicating the presence of coherent motions that are refocused by the compensated PGSE experiment. The effective diffusion coefficient from the compensated PGSE is a measure of the random particle motions on this time scale. It is asymmetric about the center of the flowing region, being larger in the lower half of the flow where deceleration occurs, in contrast to the mean velocity in the flow direction [5,6]. The data in Fig. 3(b) represent the first measurement of the spatial distribution of motion that is purely random on a specific time scale in a 3D granular shear flow.

Figure 4 shows the effective axial diffusion coefficient for $\Delta = 6.54$ ms, as a function of depth in the granular material along a line perpendicular to the free surface in the lower half of the flow. The repeated PGSE (●) and compensated PGSE (□) effective diffusion data diverge at depths shallower than $h = -7$ mm, due to the existence of axial particle motions correlated on times on the order of $\Delta = 6.54$ ms. [Images at $\Delta = 2.58$ ms to 8.66 ms show the axial diffusion coefficient still varying with Δ, indicating that $\tau_c \approx O(\Delta)$.

The effective diffusion coefficient for the repeated PGSE experiment is a maximum at the free surface ($h = 0$), like the mean velocity parallel to the free surface, shown in the inset, as measured from the phase of the signal [5]. This is a reasonable result. There should be no net axial flow in this system so all motions should be random at long enough time scale and the repeated PGSE sequence will yield the effects of random motions at all time scales.

In contrast to the repeated PGSE results, the random motions peak ~5 mm below the surface. This is an indication that the correlation time τ_c becomes longer closer to the

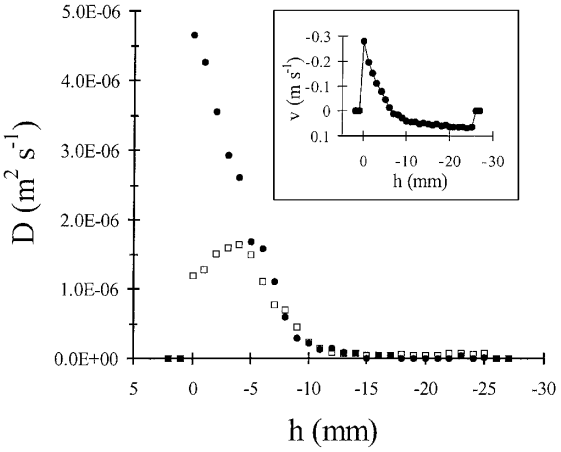

FIG. 4. Effective axial diffusion coefficient as a function of depth perpendicular to the free surface in the flowing layer at a downhill part of the flow for a rotation rate of 2.36 rad s^{-1} and displacement time $\Delta = 6.54$ ms. Compensated PGSE data (□) show a diffusion maximum below the surface while the repeated PGSE data (●) are maximal at the free surface. The divergence of the two results at shallower than -7 mm depth means there are both coherent and random axial motions over the time scale of 6.54 ms. At greater depths, all motion is random on this time scale. The inset shows the mean velocity parallel to the free surface measured along the same perpendicular line.

free surface and an ever larger fraction of them exceed Δ. On the other hand, the collisions become more frequent as the average density increases with increasing depth, but then decreases when the average flow velocity decreases at greater depth. At a depth of -13 mm the relative velocity goes to zero and D goes to a value for molecular diffusion of oil in the particles.

We have reported PGSE NMR measurements in the interior of 3D granular flows, but only in the axial direction at two isolated spots in order to show that spatial distributions of random and nonrandom motions can be separated in a specific time frame leading to the estimation of the correlation time τ_c of $O[1\ \text{ms}]$ and the velocity fluctuation intensity $\langle u^2 \rangle$ of $O[10^{-3}\ \text{m}^2\,\text{s}^{-2}]$ near the free surface. A complete study of this flow would involve measurements over a range of Δ, positions, rotation rates, and anisotropy of motion. This technique is applicable to other granular flows, regardless of the kind of interparticle interactions, provided useful NMR signals exist and the correlation times are within range of available delay time Δ. The upper limit of Δ is $\sim$200 ms, due to T_2 of these particles, while the lower limit is around a few milliseconds, at present, because of gradient hardware. An appropriate choice of material plus hardware improvements could increase this range by an order of magnitude or more.

Discussions with Professor Paul Callaghan, Dr. Sarah Codd, and Dr. Dean Keuthe are acknowledged, as is support by the Engineering Research Program of the Office of Basic Energy Sciences, Department of Energy, under Grant No. DE-FG03-98ER14912.

[1] H. M. Jaeger, S. R. Nagel, and R. P. Behringer, Rev. Mod. Phys. **68**, 1259 (1996); Phys. Today **49**, No. 4, 32 (1996).
[2] F. Melo, P. Umbanhower, and H. L. Swinney, Phys. Rev. Lett. **72**, 172 (1994); **75**, 3838 (1995).
[3] G. Metcalfe and M. Shattuck, Physica (Amsterdam) **233A**, 709 (1996); K. M. Hill, A. Caprihan, and J. Kakalios, Phys. Rev. Lett. **78**, 50 (1997).
[4] P. T. Callaghan, *Principles of Nuclear Magnetic Resonance Microscopy* (Oxford University Press, Oxford, 1991).
[5] M. Nakagawa, S. A. Altobelli, A. Caprihan, E. Fukushima, and E.-K. Jeong, Exp. Fluids **16**, 54 (1993).
[6] K. Yamane, M. Nakagawa, S. A. Altobelli, T. Tanaka, and Y. Tsuji, Phys. Fluids **10**, 1419 (1998).
[7] E. E. Ehrichs, H. M. Jaeger, J. B. Knight, G. S. Karczmar, V. Yu. Kuperman, and S. R. Nagel, Science **267**, 1632 (1995).
[8] V. Yu. Kuperman, Phys. Rev. Lett. **77**, 1178 (1996).
[9] A. Caprihan, E. Fukushima, A. D. Rosato, and M. Kos, Rev. Sci. Instrum. **68**, 4217 (1997).
[10] V. V. R. Natarajan, M. L. Hunt, and E. D. Taylor, J. Fluid Mech. **304**, 1 (1995).
[11] D. V. Kakhar, J. J. McCarthy, T. Shinbrot, and J. M. Ottino, Phys. Fluids **9**, 31 (1997).
[12] N. Menon and D. J. Durian, Phys. Rev. Lett. **79**, 3407 (1997).
[13] S. B. Savage and R. Dai, Mech. Mater. **16**, 225 (1993); S. S. Hsiau and M. L. Hunt, J. Heat Transfer **115**, 541 (1993).
[14] E. O. Stejskal and J. E. Tanner, J. Chem. Phys. **42**, 288 (1965).
[15] J. Stepisnik, Prog. Nucl. Magn. Reson. Spectrosc. **17**, 187 (1985); A. Caprihan and E. Fukushima, Phys. Rep. **198**, 195 (1990).
[16] P. T. Callaghan and J. Stepisnik, Adv. Magn. Opt. Reson. **19**, 325 (1996).
[17] R. Kubo, M. Toda, and N. Hashitsume, *Statistical Physics II: Nonequilibrium Statistical Mechanics* (Springer, Berlin, 1991).